NATURAL CONVECTION IN TILTED SQUARE CAVITIES WITH TRIANGULAR SHAPED TOP COLD WALL

Tamanna Sultana[1]*, Sumon saha[2], Goutam Saha[3] and Md. Quamrul Islam[4]
[1]Institute of Natural Science,
United International University (UIU), Dhaka-1209, Bangladesh
[2,4]Department of Mechanical Engineering,
Bangladesh University of Engineering and Technology (BUET), Dhaka-1000, Bangladesh
[3]Department of Mathematics,
University of Dhaka (DU), Dhaka-1000, Bangladesh
Email: labsachin@gmail.com

Abstract: *A numerical study of natural convection in a tilted square cavity with heated horizontal base and cold upper wall is presented. The present study is based in such a configuration where the top triangular wall of two different shapes is maintained at a constant low temperature. A constant heat flux source whose length is 20% of the total length of the cavity is discretely embedded at the left corner of the bottom wall. The remaining part of the bottom wall and the two sidewalls are considered to be adiabatic. The study includes computations for inclination angles of the cavity from 0^o to 45^o, where the Grashof number, Gr varies from 10^3 to 10^6. The Penalty finite element method has been used to see the effects of inclination angles and Grashof number on heat transfer process in the cavity. Results are presented in the form of streamline and isotherm plots as well as the variation of the average Nusselt number. Observation shows the significant effect of different triangular top surface on the heat transfer characteristics at the higher Grashof number and inclination angle.*

Keywords: *Natural convection, Penalty finite element, Nusselt number, Isoflux heating.*

INTRODUCTION

Natural convection heat transfer and fluid flow in enclosed space or closed cavities is under considerable attention of engineers because of its great importance in several thermal engineering problems. There are a variety of real-world applications of natural convection, such as, thermal insulation, cooling of electronic equipment, solar energy devices, nuclear reactors, heat-recovery systems, room ventilation, crystal growth in liquids etc. The fluid flow and heat transfer behavior of such systems can be predicted by the mass, momentum and energy conservation equations with appropriate boundary conditions. Most of the related studies are focused on differentially heated rectangular or square enclosure. However, the shape of enclosure can be in different configurations such as, in most of the related engineering situations which include triangle, parallelogram or trapezoidal and heater can be located on the bottom wall. The need for information on the thermal behavior of natural convective flow in channels and cavities has been recognized by the building design community. For example, in the case of passive solar heating and natural ventilation systems as documented by several studies. The main advantage of natural convection is its intrinsic reliability, because the air movement is simply generated by local density gradients in the presence of the gravitational field. The thermal design of a naturally ventilated device depends on geometric and operating conditions, shape and dimensions of the system, flow areas of the inlet/outlet openings, location of the heat sources, and amount of thermal power dissipated, chimney height, and so on. A great deal of these works dealing with flow and associated heat transfer in enclosures is reported in the literatures[1-4].

Natural convection in a closed square cavity has taken the center stage in many fundamental heat transfer analysis which is of prime importance in certain technological

Nomenclature

g	Gravitational acceleration
Gr	Grashof number
J	Jacobian
L	Length of the heat source
N_i	Standard shape functions
Nu	Nusselt number
p	Pressure
P	Dimensionless pressure
Pr	Prandtl number
q	Heat flux
R_i	Residual equations
T	Temperature
T_c	Temperature of the cold surface
u	Velocity component in x-direction
U	Dimensionless velocity component in X-direction
v	Velocity component in y-direction
V	Dimensionless velocity component in Y-direction
W	Width of the cavity
x, y	Cartesian co-ordinates
X, Y	Dimensionless Cartesian co-ordinates

Greek Symbols

k	Thermal conductivity of fluid
α	Thermal diffusivity
β	Coefficient of volumetric expansion
θ	Dimensionless temperature
ρ	Fluid density
ν	Kinematic viscosity
Ψ	Dependent variable
Φ	Inclination angle
γ	Penalty parameter
θ_s	Local dimensionless temperature
ΔT	Temperature difference
Ω	Element area

Subscript

c	Cold wall

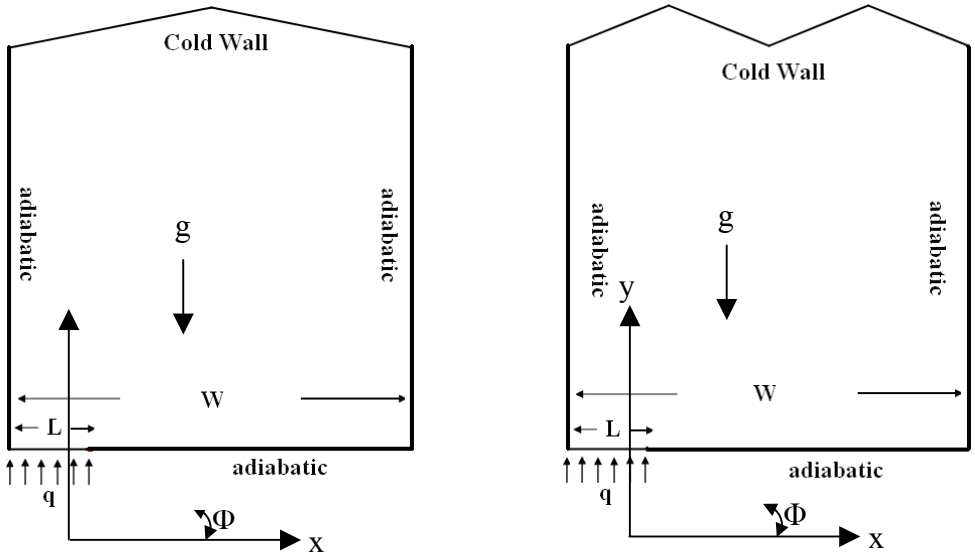

Shape 1 **Shape 2**

Figure 1: Physical models of the problem.

applications. Ali and Husain[5] investigated the natural convection heat transfer and flow characteristics in a square duct of vee corrugated vertical walls. Ali and Husain[6] also investigated the effect of corrugation frequencies on natural convective heat transfer and flow characteristics in a square enclosure of vee corrugated vertical walls. This investigation showed that the overall heat transfer through the enclosure increased with the increase of corrugation for low Grashof number; but the trend was reversed for high Grashof number. An enclosure with corrugated bottom surface maintaining a uniform heat flux and flat isothermal cooled top surface and adiabatic side walls was studied by Noorshahi *et al.*[7]. The results showed that the pseudo-conduction region was increased with the increase of the wave amplitude. Yao[8] studied theoretically the natural convection along a vertical wavy surface. Adjlout *et al.*[9] reported a numerical study of the effect of a hot wavy wall in an inclined differentially heated square cavity. Tests were performed for different inclination angles, amplitudes and Rayleigh numbers for one and three undulation. It may also be noted that the sinusoidal wall temperature variation produces uniform melting of materials such as, glass as recently reported by Sarris *et al.*[10]. In their detailed study, they described the effect of sinusoidal top wall temperature variations in a natural convection within a square enclosure where the other walls were insulated. Whereas, enclosures had been investigated to lesser extend[11,12]. Natural convection in triangular cavities had been studied in porous media by several researches[13,14]. A numerical study was carried out for the two- dimensional laminar natural convection in a pitch roof of triangular cross-section under summer day boundary condition[15]. In that work, the effects of height-base ratio and Rayleigh number on the flow structure and heat transfer were investigated. It was found that a considerable proportion of the heat transfer across the base wall of the region takes place near the intersection of the cold horizontal wall and hot inclined wall.

The present paper reports the numerical study of natural convection in a tilted square cavity (W × W) with triangular top wall where air has been taken as the working fluid. The physical model considered here are shown in Figure 1 (shape 1 and shape 2), along with the important geometric parameters. In this investigation, the top triangular wall is maintained at a constant low temperature T_c, a constant heat flux source, q of length L = 0.2W is discretely embedded at the left corner of the bottom wall, and the remaining non-heated parts of the bottom surface and the two vertical sidewalls are considered to be adiabatic. Two different shapes are considered where shape 1 and shape 2 have one and two triangular tops respectively with the same amplitude fixed at 10% of the cavity length. In the present study, numerical simulations are carried out for different inclination angles with Gr = 10^3 to 10^6 and a fixed Prandtl number, Pr of 0.71.

GOVERNING EQUATIONS

Consider a steady two-dimensional laminar flow of incompressible fluid, with negligible viscous dissipation effect. For the treatment of the bouncy term in the momentum equation, Boussinesq approximation is adopted to account for the variations of temperature as a function of density, and to couple in this way the temperature field to the flow field. Then the governing equations for steady natural convection flow using conservation of mass, momentum and energy can be expressed in the dimensionless form as:

$$\frac{\partial U}{\partial X}+\frac{\partial V}{\partial Y}=0 \quad (1)$$

$$U\frac{\partial U}{\partial X}+V\frac{\partial U}{\partial Y}=-\frac{\partial P}{\partial X}+\Pr\left[\frac{\partial^2 U}{\partial X^2}+\frac{\partial^2 U}{\partial Y^2}\right]+(\mathrm{Gr}\,\Pr\sin\Phi)\,\theta \quad (2)$$

$$U\frac{\partial V}{\partial X}+V\frac{\partial V}{\partial Y}=-\frac{\partial P}{\partial Y}+\Pr\left[\frac{\partial^2 V}{\partial X^2}+\frac{\partial^2 V}{\partial Y^2}\right]+(\mathrm{Gr}\,\Pr\cos\Phi)\,\theta \quad (3)$$

$$U\frac{\partial \theta}{\partial X}+V\frac{\partial \theta}{\partial Y}=\frac{\partial^2 \theta}{\partial X^2}+\frac{\partial^2 \theta}{\partial Y^2} \quad (4)$$

where, U and V are the velocity components in the X and Y directions, respectively, θ is the temperature, P is the

pressure and Φ is the inclination angle of the enclosure. The Grashof number and the Prandtl number are defined as:

$$Gr = \frac{g\beta\Delta T W^3}{\nu^2} \text{ and } Pr = \frac{\upsilon}{\alpha} \tag{5}$$

The dimensionless parameters in the equations above are defined as follow:

$$X = \frac{x}{W}, Y = \frac{y}{W}, U = \frac{uW}{\upsilon}, V = \frac{vW}{\upsilon},$$
$$P = \frac{pW^2}{\rho\upsilon^2}, \theta = \frac{T - T_c}{\Delta T} \text{ and } \Delta T = \frac{qW}{k} \tag{6}$$

where, ρ, β, υ, α and g are the fluid density, coefficient of volumetric expansion, kinematic viscosity, thermal diffusivity, and gravitational acceleration respectively. The corresponding boundary conditions for the above problem

$$U\frac{\partial U}{\partial X} + V\frac{\partial V}{\partial Y} = \gamma\frac{\partial}{\partial X}\left(\frac{\partial U}{\partial X} + \frac{\partial V}{\partial Y}\right) + Pr\left(\frac{\partial^2 U}{\partial X^2} + \frac{\partial^2 U}{\partial Y^2}\right) + \left(Ra\, Pr \sin\Phi\right)\theta \tag{10}$$

$$U\frac{\partial V}{\partial X} + V\frac{\partial V}{\partial Y} = \gamma\frac{\partial}{\partial Y}\left(\frac{\partial U}{\partial X} + \frac{\partial V}{\partial Y}\right) + Pr\left(\frac{\partial^2 V}{\partial X^2} + \frac{\partial^2 V}{\partial Y^2}\right) + \left(Ra\, Pr \cos\Phi\right)\theta \tag{11}$$

Expanding the velocity components (U, V) and temperature (θ) using basis set $\{N_k\}_{k=1}^{N}$ as

$$U \approx \sum_{k=1}^{N} U_k N_k, V \approx \sum_{k=1}^{N} V_k N_k, \text{and } \theta \approx \sum_{k=1}^{N} \theta_k N_k \tag{12}$$

Then the Galerkin finite element method yields the following nonlinear residual equations for Eqs. (10), (11), and (12) respectively at nodes of internal domain A.

$$R_i^{(1)} = \sum_{k=1}^{N} U_k \int_\Omega \left[\left(\sum_{k=1}^{N} U_k N_k\right)\frac{\partial N_k}{\partial X} + \left(\sum_{k=1}^{N} V_k N_k\right)\frac{\partial N_k}{\partial Y}\right] N_i dXdY + \gamma\left[\sum_{k=1}^{N} U_k \int_\Omega \left(\frac{\partial N_i}{\partial X}\frac{\partial N_k}{\partial X}\right) dXdY + \sum_{k=1}^{N} V_k \int_\Omega \left(\frac{\partial N_i}{\partial Y}\frac{\partial N_k}{\partial Y}\right) dXdY\right] \tag{13}$$
$$+ Pr \sum_{k=1}^{N} U_k \int_\Omega \left(\frac{\partial N_i}{\partial X}\frac{\partial N_k}{\partial X} + \frac{\partial N_i}{\partial Y}\frac{\partial N_k}{\partial Y}\right) dXdY - \left(Ra\, Pr \sin\Phi\right)\int_\Omega \left(\sum_{k=1}^{N} \theta_k N_k\right) N_i dXdY$$

$$R_i^{(2)} = \sum_{k=1}^{N} V_k \int_\Omega \left[\left(\sum_{k=1}^{N} U_k N_k\right)\frac{\partial N_k}{\partial X} + \left(\sum_{k=1}^{N} V_k N_k\right)\frac{\partial N_k}{\partial Y}\right] N_i dXdY + \gamma\left[\sum_{k=1}^{N} U_k \int_\Omega \left(\frac{\partial N_i}{\partial Y}\frac{\partial N_k}{\partial X}\right) dXdY + \sum_{k=1}^{N} V_k \int_\Omega \left(\frac{\partial N_i}{\partial Y}\frac{\partial N_k}{\partial X}\right) dXdY\right] \tag{14}$$
$$+ Pr \sum_{k=1}^{N} V_k \int_\Omega \left(\frac{\partial N_i}{\partial X}\frac{\partial N_k}{\partial X} + \frac{\partial N_i}{\partial Y}\frac{\partial N_k}{\partial Y}\right) dXdY - \left(Ra\, Pr \cos\Phi\right)\int_\Omega \left(\sum_{k=1}^{N} \theta_k N_k\right) N_i dXdY$$

$$R_i^{(3)} = \sum_{k=1}^{N} \theta_k \int_\Omega \left[\left(\sum_{k=1}^{N} U_k N_k\right)\frac{\partial N_k}{\partial X} + \left(\sum_{k=1}^{N} V_k N_k\right)\frac{\partial N_k}{\partial Y}\right] dXdY + \sum_{k=1}^{N} \theta_k \int_\Omega \left(\frac{\partial N_i}{\partial X}\frac{\partial N_k}{\partial X} + \frac{\partial N_i}{\partial Y}\frac{\partial N_k}{\partial Y}\right) dXdY \tag{15}$$

are given by:

For all walls: $U = V = 0$,
At top wall: $\theta = 0$,
In Right and left side walls: $\frac{\partial\theta}{\partial Y} = 0$
For bottom wall: $\frac{\partial\theta}{\partial Y} = \begin{cases} 0 & \text{for } 0.2 < X < 1 \\ -1 & \text{for } 0 \le X \le 0.2 \end{cases}$ (7)

The average Nusselt number can be written as,

$$Nu = \frac{1}{0.2}\int_0^{0.2} \frac{1}{\theta_S(X)} dX \tag{8}$$

where, $\theta_S(X)$ is the local dimensionless temperature of the heated surface. The Simpson's rule is used for numerical integration to obtain the average Nusselt number.

FINITE ELEMENT FORMULATION

The continuity equation (1) can be used as a constraint due to mass conservation and this constraint may be used to obtain the pressure distribution. In order to solve Eqs. (2) to (4), the Penalty finite element method[16] has been used where the pressure P is eliminated by a penalty parameter γ and the incompressibility criteria is given by Eq. (1) which results in:

$$P = -\gamma\left(\frac{\partial U}{\partial X} + \frac{\partial V}{\partial Y}\right) \tag{9}$$

The continuity Eq. (1) is automatically satisfied for large values of γ. Using Eq. (9), the momentum Eqs. (2) and (3) reduces to

Three point Gaussian quadrature formula is used to evaluate the integrals in the residual equations. The non-linear residual Eqs. (13) to (15) are solved using Newton's method to determine the coefficients of the expansions in Eq. (12). Also

$$X = \sum_{k=1}^{6} X_k N_k(\xi,\eta) \text{ and } Y = \sum_{k=1}^{6} Y_k N_k(\xi,\eta) \tag{16}$$

where, $N_i(\xi, \eta)$ are the local six noded triangular basis functions on the $\xi - \eta$ domain. The integrals in Eqs. (13) to (15) can be evaluated in ξ - η domain using following relationships:

$$\begin{bmatrix} \frac{\partial N_i}{\partial X} \\ \frac{\partial N_i}{\partial Y} \end{bmatrix} = \frac{1}{J}\begin{bmatrix} \frac{\partial Y}{\partial \eta} & -\frac{\partial Y}{\partial \xi} \\ -\frac{\partial X}{\partial \eta} & \frac{\partial X}{\partial \xi} \end{bmatrix}\begin{bmatrix} \frac{\partial N_i}{\partial \xi} \\ \frac{\partial N_i}{\partial \eta} \end{bmatrix} \text{ and } dX\, dY = J\, d\xi\, d\eta \tag{17}$$

$$J = \frac{\partial(X,Y)}{\partial(\xi,\eta)} = \begin{vmatrix} \frac{\partial X}{\partial \xi} & \frac{\partial X}{\partial \eta} \\ \frac{\partial Y}{\partial \xi} & \frac{\partial Y}{\partial \eta} \end{vmatrix} \tag{18}$$

NUMERICAL PROCEDURE

The numerical procedure used to solve the governing equations for the present work is the Penalty finite element method. The application of this technique is well documented by Zienkiewicz and Taylor[17]. It provides the smooth solutions at the interior domain including the corner regions. The non-linear parametric solution method is chosen to solve the finite element equations. This

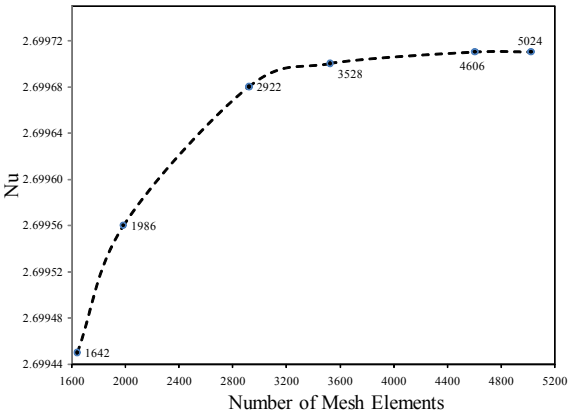

Figure 2: Grid refinement test.

approach will result in substantially fast convergence assurance. A non-uniform triangular mesh arrangement is implemented in the present investigation especially near the heated surface to capture the rapid changes in the dependent variables. Also six noded triangular elements are used in this paper since the six noded elements smoothly capture the non-linear variations of the field variables. All six nodes are associated with velocities as well as temperature, only the corner nodes are associated with pressure. Solutions are assumed to converge when the following convergence criteria is satisfied for every dependent variables at every point in the solution domain

$$\left|\frac{\Psi_{new}-\Psi_{old}}{\Psi_{old}}\right| \le 10^{-6} \qquad (19)$$

where, Ψ represents a dependent variable U, V, P, and θ.

GRID REFINEMENT CHECK

The grid-independent test has been performed at Pr = 0.71 and Gr = 10^3 for the configuration of a single triangular top as reported in Figure 2. Extensive numerical tests are performed and it is found that 4606 mesh elements provides satisfactory results for the test geometry and the solution obtained is to be independent of the grid size. In order to validate the numerical model, the results are compared with those reported by Sharif and Mohammad[18], for square straight enclosure with Gr = 10^6 and L/W = 0.4 as shown in Figure 3. The agreement is found to be excellent which validates the present computations indirectly.

RESULTS AND DISCUSSION

A parametric study is carried out to examine the effect of inclination angles of the two different triangular top enclosures for Grashof number, Gr = 10^3, 10^4, 10^5 and 10^6. In this investigation, working fluid is chosen as air with the Prandtl number, Pr = 0.71.

The main characteristics of the flow and the energy transport for two different triangular top square cavity are shown in the Figures 4, 5, 6 and 7 in terms of streamlines and isotherms respectively for various Gr = 10^3 and 10^6. Since the heated part of the bottom wall is at a higher temperature than the top wall, the density of fluid near the left corner of the bottom wall decreases compared to the density of the fluid adjacent to the top wall. As a result, the flow rises along the left vertical wall and gets blocked at the top cold wall, which turns the flow horizontally towards the adiabatic right wall. The flow then descends downwards and turns back horizontally to the left heated region after hitting the bottom wall. Thus the flowing fluid forms clockwise rotations inside the cavity as seen from those figures. It is observed that for Grashof number, Gr ≤ 10^4, the convection effect is very less between the walls. With the increase of Gr, the buoyancy force increases, resulting in a strong circulation of the fluid inside the cavity and thus indicating convective heat transport.

Figure 4 shows the variation of streamlines and isotherm plots for one triangular top square cavity with Gr = 10^4. It is shown from the figure that the velocity profiles of the enclosure are denser near the side walls and a core is observed at the center position of the enclosure. This is due to the geometry of top wall. In presence of the lower magnitude of Grashof number, the formation of circulating cell at Φ = 0° is almost symmetry about the center line of enclosure. At Φ = 15°, that is, increasing the inclination angle the circulating cell slightly inclined from left to right and the core seems to move downward. But at Φ = 30°, the cell comes into the symmetry position again and the presence of core seems at the center region of the enclosure. At Φ = 45°, the streamline plots exhibits the same nature. At higher Grashof number, when the intensity of convection increases significantly, the core of the

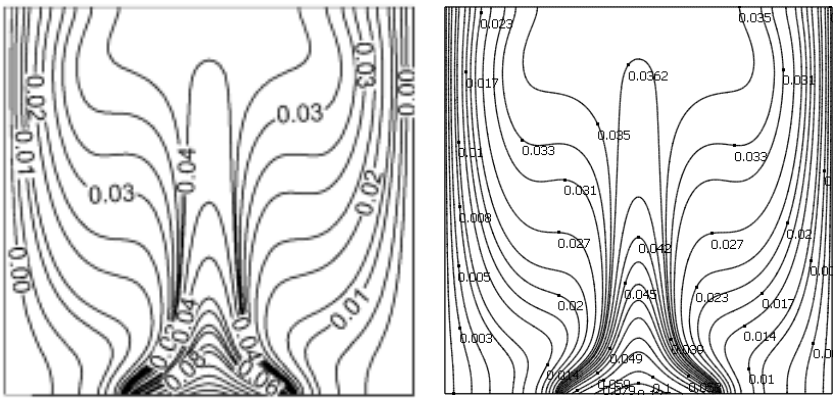

Sharif and Mohammad[18] Present Work

Figure 3: Comparison of the Isotherm plots of the square straight enclosure with Sharif and Mohammad[18] at Gr = 10^6 and L/W = 0.4

circulating rolls moves up. It is observed that in the presence of the higher magnitude of Grashof number, Gr = 10^6, as the inclination angle increases, the circulating cell slanting from right to left. This phenomenon is shown in Figure 5.

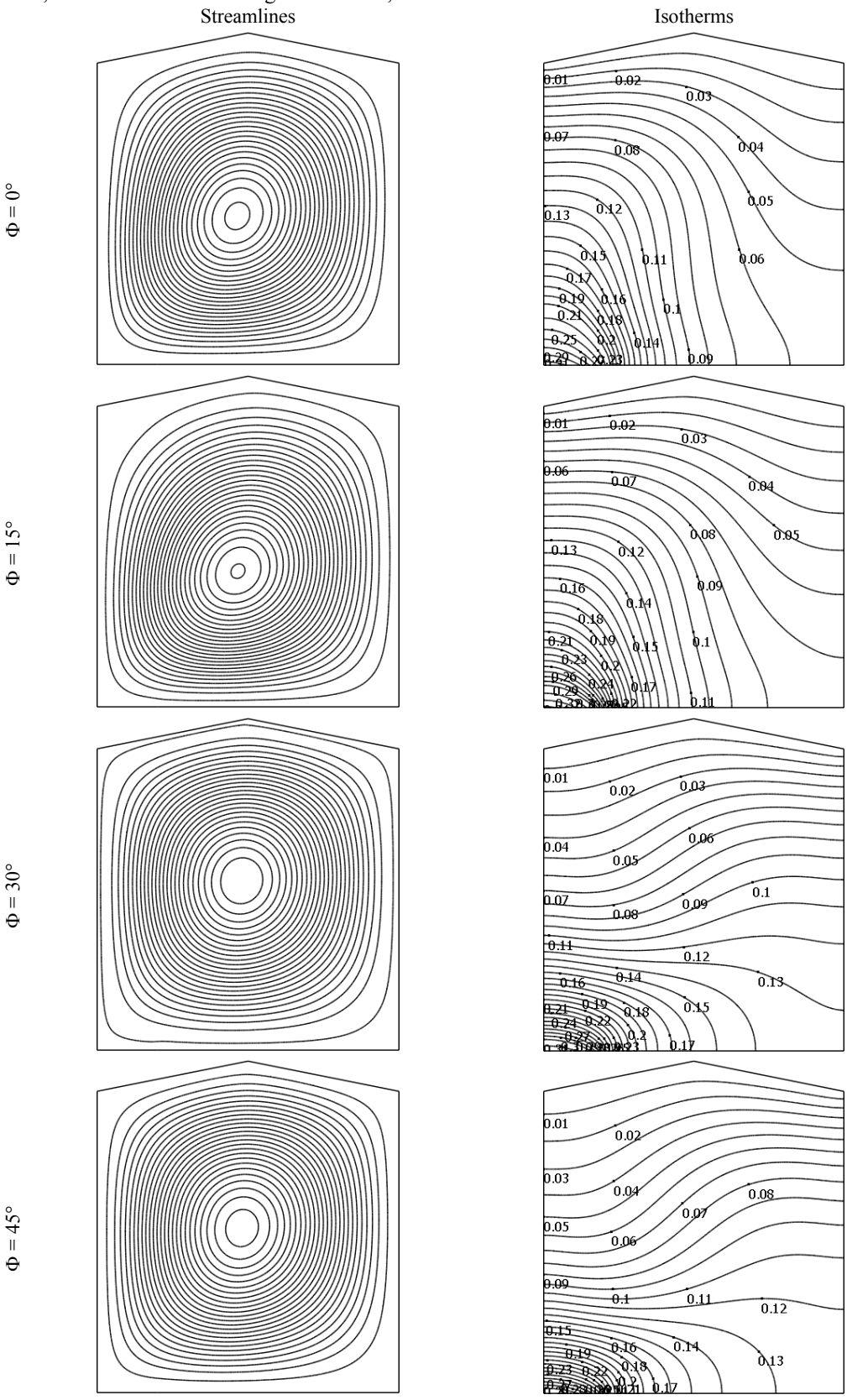

Figure 4: Variation of streamline and Isotherm plots for shape 1 with Gr = 10^4

The nature of isotherm plot for Grashof number, Gr = 10^4 and 10^6 are shown in Figures 4 and 5 respectively. It is found that for different inclination angles the temperature decreases uniformly from the heated part of the bottom wall to the top wall. The temperature contours are highly dense near the bottom wall and concentrates towards the hot surface indicating the presence of large temperature gradient there. At higher Grashof number, Gr = 10^6, the isotherm

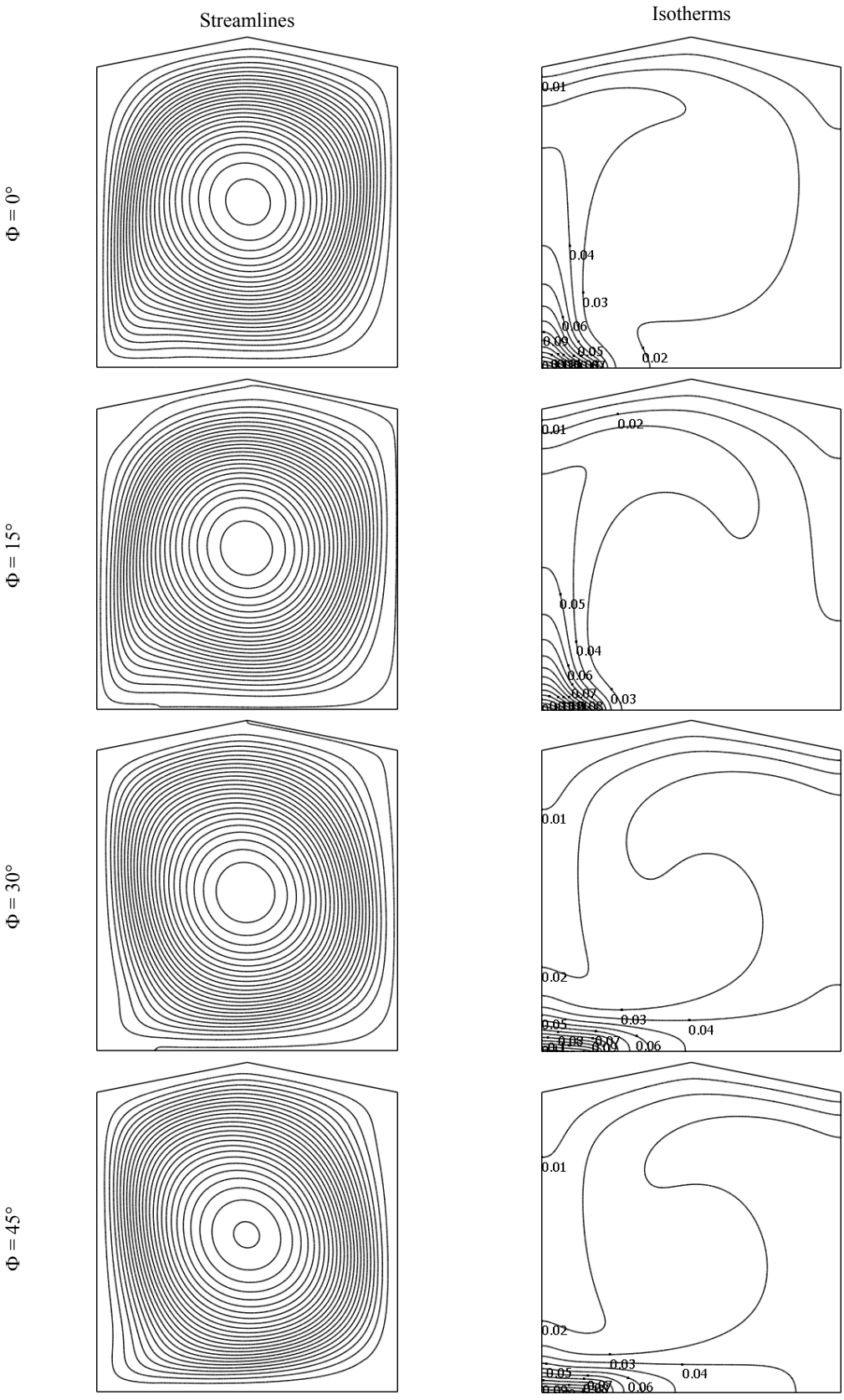

Figure 5: Variation of streamline and Isotherm plots for shape 1 with Gr = 10^6

patterns changes significantly indicating that the advection is the dominating heat transfer mechanism in the enclosure. It is observed that as the inclination angle increases, some of the temperature contours occur near the top wall and a non-uniform oval shape profiles are visualized at the center region which cover the full region of the enclosure.

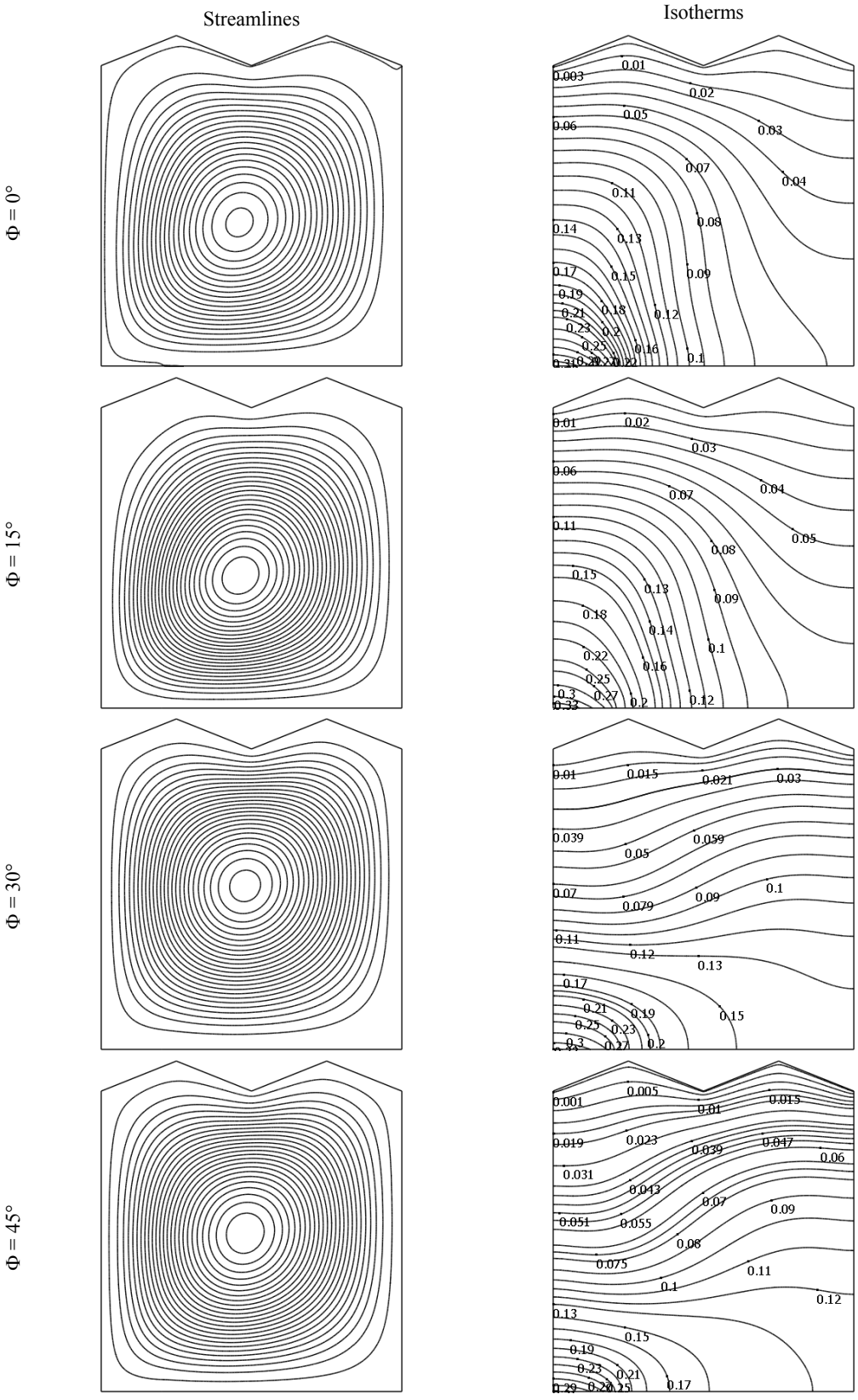

Figure 6: Variation of streamline and Isotherm plots for shape 2 with Gr = 10^4

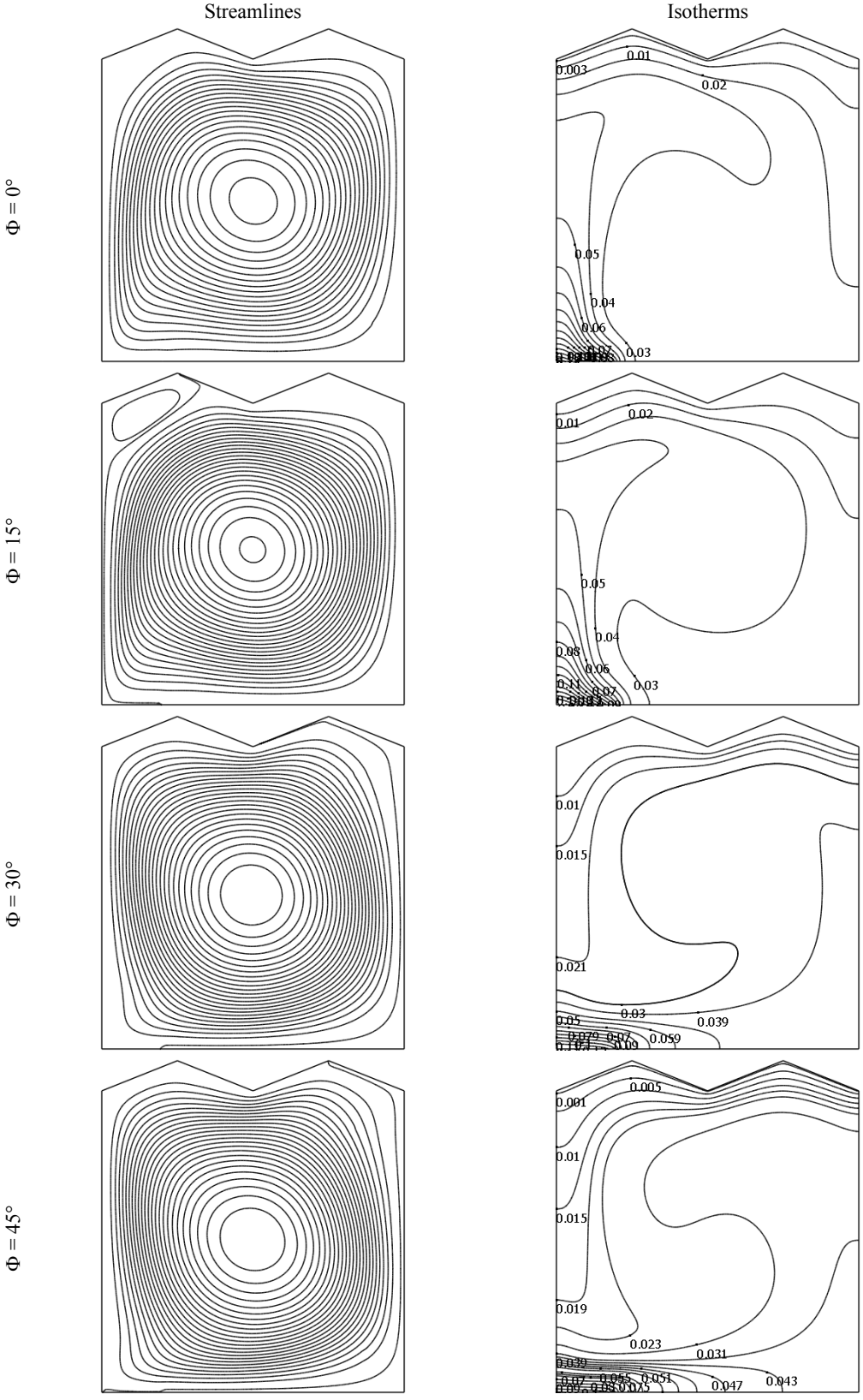

Figure 7: Variation of streamline and Isotherm plots for shape 2 with Gr = 10^6

The variation of streamline and isotherm plots for two triangular top shaped square cavities are shown in Figures 6 and 7 for lower and higher magnitude of Grashof number. The visual examination of stream lines are almost same. For large Grashof number, Gr = 10^6, there exists a small vortex near the left corner of the triangular top at inclination angle Φ = 15°. As the inclination angle increases, the isotherms plots

become denser near the hotter region and some oval shape profiles cover the full region of the enclosure. This phenomenon is visualized in Figure 7.

The variation of the average Nusselt number with Grashof number, Gr, are investigated for the different inclination angles, Φ, which are shown in Figure 8(a, b). In general, the Nusselt number increases with the increase of Grashof number. It is observed that for lower Grashof number ($Gr \leq 10^4$), the average Nusselt number increases slightly with increasing value of Gr for both shape 1 and shape 2 for different inclination angle, Φ. This phenomenon indicates the fact that buoyancy effect does not dominate the heat transport mechanism for small value of Gr. As the Grashof number increases, the heat transfer rate increases more rapidly comparing to the shape 2. It is also found that the maximum heat transfer occurs only for shape 1 when the inclination angle is $\Phi = 0°$. The reason behind this phenomenon is that with the increase of isothermal surface at the top wall, heat transfer rate grows up for single triangular top at higher Gr. Moreover, for double triangular tops, the development of local eddies on each top corner of the triangles reduce the heat transfer process though further increase of heat transfer surfaces.

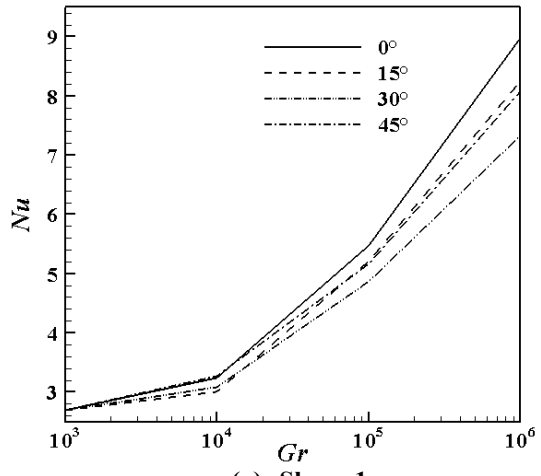

(a) Shape 1

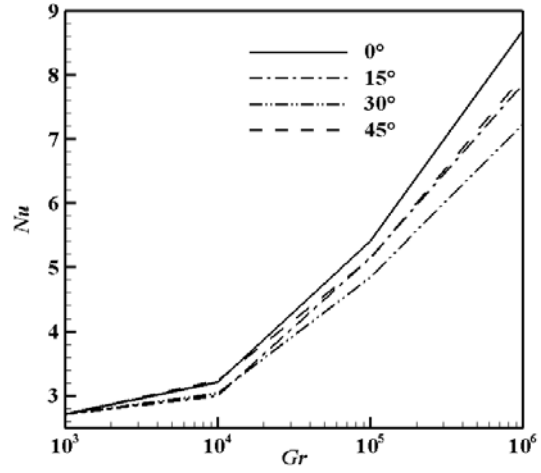

(b) Shape 2

Figure 8: Average Nusselt number variation with Gr for different inclination angles, Φ

CONCLUSION

In this investigation, natural convective of a localized constant heat flux embedded at the left side of the bottom wall of a tilted square cavity where the sidewalls are adiabatic and the modified top wall is isothermal have been investigated and analyzed numerically using the penalty finite element method for $Gr = 10^3$ to 10^6 and $Pr = 0.71$. The above analysis shows the effect of inclination angle for different Grashof number for natural convection inside a different triangular top square cavity. The brief summery of the results can be mentioned below:

i) The flow rises along the left vertical wall and gets blocked at the top cold wall, which turns the flow horizontally towards the adiabatic right wall. The flow then descends downwards and turns back horizontally to the left heated region after hitting the bottom wall. Thus the flowing fluid forms clockwise rotations inside the cavity.

ii) Comparing the results of the different shapes with lower Grashof number, the maximum Nusselt number obtained for $\Phi = 0°$ which is significantly different from other inclination angle.

iii) For $Gr \leq 10^4$, there is a very little change in Nusselt number for all inclination angles for different shapes.

iv) The maximum heat transfer occurs only for shape 1 when the inclination angle is $\Phi = 0°$.

REFERENCES

[1] Raithby, G. D., Hollands, K. G. T., 1985, "Natural Convection", in: W. M. Rohsenow, J. P. Hartnett, E. N. Ganic (Eds.), Handbook of Heat Transfer Fundamentals, 2nd Edition, McGraw-Hill, New York.

[2] Ostrach, S., 1988, "Natural Convection in Enclosures", J. Heat Transfer, Vol. 110, pp. 1175-1190.

[3] Selamet, E. E., Arpaci, V. S., Borgnakke, C., 1992, "Simulation of Laminar Buoyancy-driven Flows in an Enclosure", Numer. Heat Transfer, Part A, Vol. 22, pp. 401-420.

[4] Ravi, M. R., Henkes, R. A. W., Hoogendoorn, C. J., 1994, "On the High-Rayleigh Number Structure of Steady Laminar Natural-Convection Flow in a Square Enclosure", J. Fluid Mech., Vol. 262, pp. 325-351.

[5] Ali, M. and Husain, S. R., 1992, "Natural Convection Heat Transfer and Flow Characteristics in a Square Duct of V-Corrugated Vertical Walls", J. of Energy, Heat & Mass Transfer, Vol. 14, pp. 125-131.

[6] Ali, M. and Husain, S. R., 1993, "Effect of Corrugation Frequencies on Natural Convective Heat Transfer & Flow Characteristics in a Square Enclosure of Vee-Corrugated Vertical Walls", Int. J. of Energy Research, Vol. 17, pp. 697-708.

[7] Noorshahi, S., Hall, C., Glakpe, E., 1992, "Effect of Mixed Boundary Conditions on Natural Convection in an Enclosure with a Corrugated Surface", in: ASME-JSES-KSES Int. Solar Energy Conference Part 1, Maui, HI, pp. 173-181.

[8] Yao, L. S., 1983, "Natural Convection along a Vertical Wavy Surface", J. Heat Transfer, Vol. 105, pp. 465-468.

[9] Adjlout, L., Imine, O., Azzi, A., and Belkadi, M., 1997, "Numerical Study of the Natural Convection in a Cavity with Undulated Wall", in: Third International Thermal Energy and Environment Congress, Merrakech, Maroc, pp. 9-12.

[10] Sarris, I. E., Lekakis, I., Vlachos, N. S., 2002, "Natural Convection in a 2D Enclosure with Sinusoidal Upper Wall Temperature", Numer. Heat Transfer, Part A, Vol. 42, pp. 513–530.

[11] Lee, J. H., Lee, T. S., 1981, "Natural Convection in the Annuli between Horizontal Confocal Elliptic Cylinders", Int. J. Heat Mass Transfer, Vol. 24, pp. 1739.

[12] Akinsete, V. A., Coleman, T. A., 1982, "Heat Transfer by Steady Laminar Free Convection in Triangular Enclosures", Int. J. Heat Mass Transfer, Vol. 25, pp. 991.

[13] Philip, J. R., 1982, "Free Convection at Small Rayleigh Number in Porous Cavities of Rectangular, Elliptical, Triangular and Other Cross-Sections", Int. J. Heat Mass Transfer, Vol. 25, pp. 1503-1509.

[14] Baytas, A. C., Pop, I., 1999, "Free Convection in Oblique Enclosure Filled with a Porous Medium", Int. J. Heat Mass Transfer, Vol. 42, pp. 1047-1057.

[15] Asan, H., Namli, L., 2000, "Laminar Natural Convection in a Pitched Roof Triangular Cross-Section", Energy Build. Vol. 33, pp. 69-73.

[16] Basak, T., Roy, S., and Balakrishnan, A. R., 2006, "Effects of Thermal Boundary Conditions on Natural Convection Flows within a Square Cavity", Int. J. Heat Mass Transfer, Vol. 49, pp. 4525–4535.

[17] Zienkiewicz, O. C., Taylor, R. L., 2000, "The Finite Element Method", 5th Edn. Oxford: Butterworth-Heinemann.

[18] Sharif, A. R. and Mohammad, T. R., 2005, "Natural Convection in Cavities with Constant Flux Heating at the Bottom Wall and Isothermal Cooling from the Sidewalls", Int. J. Thermal Sciences, Vol. 44, 865-878.